



Research article

Design and fabrication of highly thermally conductive 1-1-3 piezoelectric composites

Zhiyang Liu^a, Zhiwei Zhang^{a,b,c,**}, Lei Qin^{a,b,c,*}^a Beijing Key Laboratory for Sensors, Beijing Information Science & Technology University, Beijing, 100192, China^b Key Laboratory of Modern Measurement and Control Technology, Ministry of Education, Beijing Information Science & Technology University, Beijing, 100192, China^c Beijing Key Laboratory for Optoelectronic Measurement Technology, Beijing Information Science & Technology University, Beijing, 100192, China

ARTICLE INFO

Keywords:

Thermal conduction
1-1-3 piezoelectric composite
Heat dissipation structure
Finite element analysis

ABSTRACT

1-3 piezoelectric composites have been widely used in transmitting transducers, medical devices, navigation, aerospace, etc. However, due to poor thermal conduction of inside piezoelectric composites, performance degradation and service life shortening of transmitting transducers are easily caused while working under high-power or continuously operated states. In this paper, a solution is provided by designing and creating highly efficient thermally conductive paths in 1-1-3 piezoelectric composite. This novel design resulted in two-fold increase in heat dissipation rate compared with traditional 1-3 piezoelectric composites, while maintaining high piezoelectric properties. Furthermore, we designed and fabricated an efficient heat dissipation transducer (EHDT) with the novel 1-1-3 piezoelectric composite as the core material, which can relief heat accumulation effectively compared with conventional transducers (CT). The EHDT can achieve three times more power output than the CT at the same temperature threshold of 90 °C.

1. Introduction

Traditional 1-3 piezoelectric composites have been widely used in underwater transducers, medical devices, navigation and aerospace [1-4], especially as the important part of high-frequency acoustic emission transducers [5-9]. These high-frequency transducers are usually operated continuously with high power. Under such conditions, traditional 1-3 piezoelectric composites become bottleneck for high-frequency and high-power transmitting transducers, because continuous operation of the devices under such conditions can elevate the internal temperature of the transducers gradually and lead to electric domain flipping in piezoelectric ceramic. This phenomenon increases piezoelectric and dielectric constants while decreasing residual polarization and residual strain or permanent depolarization failure if the temperature exceeds the Curie temperature (T_c) of piezoelectric ceramic [10,11]. In view of the rigorous requirements of high-frequency and high-power transmitting transducers for prolonged operation at elevated temperatures, it is essential to develop new piezoelectric composites exhibiting low loss and high thermal conductivity. However, up to now researchers primarily focused on lowering the loss, but with little attention to increase thermal conductivity of piezoelectric composites [12,13].

Heat dissipation, rather than solely decreasing the dielectric loss of piezoelectric ceramics, is a more practical approach to optimize

* Corresponding author. Beijing Key Laboratory for Sensors, Beijing Information Science & Technology University, Beijing, 100192, China.

** Corresponding author. Beijing Key Laboratory for Sensors, Beijing Information Science & Technology University, Beijing, 100192, China.

E-mail addresses: zhiweizhang@bistu.edu.cn (Z. Zhang), qinlei@bistu.edu.cn (L. Qin).

the performance of transducers. Therefore, the present study mainly focuses on design and optimization of heat dissipation in piezoelectric transducers. For example, Li et al. conducted experiments on heat dissipation of PZT piezoelectric ceramic circular plates of 10 mm diameter and 3 mm thickness [14]. The study revealed that when a cooling water system was applied to the outer surface, surface temperature of the piezoelectric ceramic disk could be maintained at about 20 °C during its high-power continuous operation. However, the core temperature of the disk remained as high as 200 °C, which is close to the Curie temperature of the piezoelectric ceramic. This high temperature led to a significant loss in the actuation performance of the device. To address the heat dissipation bottleneck, Shan from Peking University introduced an innovative design by incorporating vertical graphene/ceramic hybrid heat sinks into the transducer, which significantly reduced the operating temperature [15]. Other researchers have also focused on designing heat dissipation structures for the outer shell of the transducers. However, all these designs remained ineffective in optimizing the core temperature of the piezoelectric composite, thus having limited utilization for complete heat dissipation [16–18].

Here, we explored and analyzed the composition and internal structure of piezoelectric composites for efficient heat transfer. Then a novel high thermally conductive 1-1-3 piezoelectric composite was designed and fabricated. The novel material combined with well-designed heat sinks can achieve efficient heat dissipation to meet the demands of high-frequency and high-power transmitting transducers.

2. Structural design and analysis

In conventional 1–3 piezoelectric composite, as shown in Fig. 1(a), both the piezoelectric ceramic and epoxy resin are insulating materials with limited thermal conductivity. Additionally, the maximum stress appears in the center of the piezoelectric ceramics, which vibrates at k_{33} mode. Along with mechanical loss and dielectric loss, the energy that cannot be converted increases the internal energy of piezoelectric ceramics. So, the heat transfer path, as shown in Fig. 1(b)—is mainly along with the piezoelectric ceramic from center to the up and down surfaces. And a small part of heat is also transferred to the epoxy resin. The process is conducted by phonon vibrations within the composite, which is an inefficient heat conduction. As such, it makes heat dissipation difficult, and the transducer's temperature continues to rise during high-frequency, high-power operation until the failure of the device [19,20].

On the other hand, the novel 1-1-3 piezoelectric composite introduced in the present study comprises piezoelectric ceramic, silicone rubber, and an aluminum alloy frame, as shown in Fig. 1(c). The alloy frame is designed to replace the epoxy resin in 1–3 piezoelectric composite. Silicone rubber with high thermal conductivity has been added between the alloy frame and the piezoelectric ceramic to fixed the whole composite together, using electrons inside metals to achieve rapid heat conduction. In this way, the heat transfer path, as shown in Fig. 1(d)—is changed in the novel configuration. Heat will transfer horizontally to the silicon rubber first, then move to the aluminum alloy frame and finally to the surfaces vertically through the highly conducting metal frame.

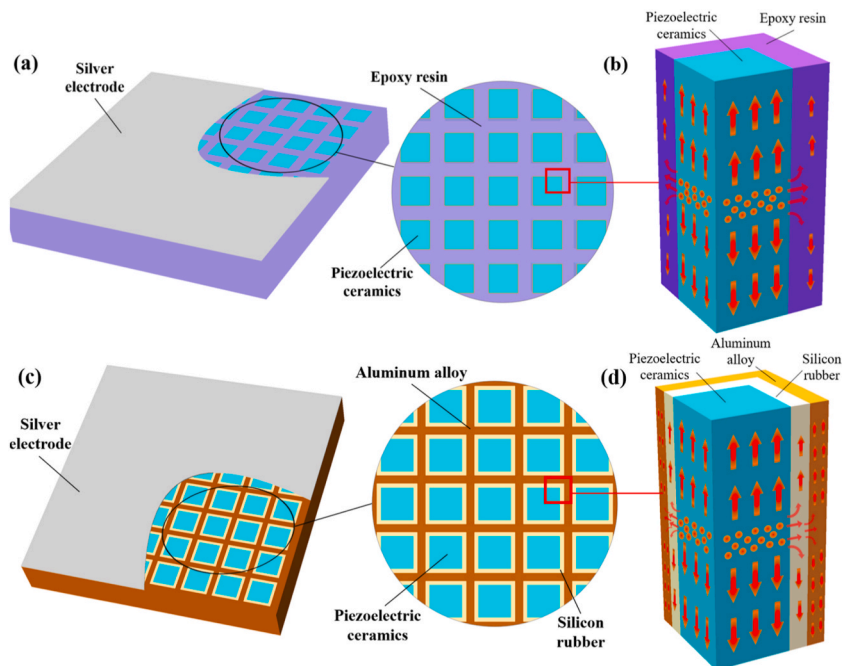


Fig. 1. Schematic illustration of the structures of different piezoelectric composites and the Internal heat transfer pathways (a) structure of conventional 1–3 piezoelectric composite (b) Internal heat transfer pathway of conventional 1–3 type, (c) structure of novel 1-1-3 piezoelectric composite, (d) Internal heat transfer pathway of novel 1-1-3 type.

3. Finite element analysis

Finite element analysis of the designed 1-1-3 piezoelectric composite was performed to simulate the piezoelectricity and heat transfer of the composite using ANSYS software. APDL command flow of the software was used to input analysis properties, material parameters (Table 1 and Table 2), model of the 1-1-3 piezoelectric composite, meshing, loads, and boundary conditions.

The simulated electrical conductivity and admittance of 1-1-3 piezoelectric composite are shown in Fig. 2. These results indicated that resonant frequency, anti-resonant frequency, and electromechanical coupling coefficient k_t of the material were approximately 330 kHz, 436 kHz, and 0.654, respectively. Compared to the results of the 1–3 piezoelectric composite obtained by other researchers, it can be concluded that the difference between the piezoelectric performance of the two composites was minimal [21–25]. Thus, the impact of the new structure on the electromechanical performance of the composite was insignificant.

The magnitude of displacements of each part of the piezoelectric composite was obtained at the resonant frequency of 330 kHz. As shown in Fig. 3, when the composite vibrated at the resonant frequency, the displacement of the piezoelectric ceramic was the maximum, and that of the silicone rubber was hierarchical, with more significant displacement in the region closely adjacent to the ceramic column. The simulation results, structure addition of aluminum alloy frame has little effect on the electrical resonance and mechanical vibration characteristics of the composite.

To analyze heat transfer, a temperature of 80 °C was applied to the center of different piezoelectric ceramic columns for a set time and step size and the resulting temperature distribution contour maps were obtained, as shown in Fig. 4. From Fig. 4(a), it is evident that the temperature within 1–3 piezoelectric composite was predominantly concentrated in the central part of the ceramic, with limited heat conduction to the horizontal surface. Moreover, the lowest temperature point was observed at the outermost surface of the epoxy resin. Conversely, in Fig. 4(b), the temperature distribution of the 1-1-3 piezoelectric composite revealed the lowest temperature point transfer to the surface of piezoelectric ceramic. It suggests most of the heat transferred through the aluminum alloy framework. Furthermore, in Fig. 4(c), with an enhanced thermal conductivity of the silicone rubber, the temperature distribution demonstrated improved performance, notably increasing on the surface.

Thus, by increasing the thermal conductivity of silicone rubber, it could be analyzed from the temperature distribution contour maps that the temperature on the surface of the piezoelectric composite gradually increased (Fig. 5), indicating more efficient heat transfer from the interior to the surroundings.

4. Experimental

Compared to epoxy, silicone rubber possesses a lower Young's modulus and higher Poisson's ratio, (Young's modulus and Poisson's ratio of epoxy resin and silicone rubber: $6.3 \times 10^9 \text{ N m}^{-2}$, 0.3; $2.55 \times 10^6 \text{ N m}^{-2}$, 0.49) reducing lateral vibration coupling in 1–3 piezoelectric composite and thus enhancing the electromechanical coupling coefficient [26,27]. However, it has a lower thermal conductivity, which can impact the overall thermal conduction rate of the piezoelectric composite. Thermally conductive fillers are the critical component of modified adhesives, with current research focusing on their development, modification, and blending with the polymer matrix. Various ceramics, such as highly thermally conductive silicon carbide, aluminum nitride, boron nitride, and aluminum oxide particles, are used in thermally conductive adhesive formulations [28,29].

Increasing the conductive filler content in the matrix is an effective way to enhance its thermal conductivity. However, an inappropriate filling may affect the composites' rheological and mechanical properties. So, choosing a reasonable particle size and volume fraction can build a much denser thermal paths along the heat transfer direction, which will improve the heat transfer efficiency and also maintain good mechanical properties. As shown in Fig. 6, the thermally conductive adhesive used in 1-1-3 piezoelectric composite was required to establish as many and as short effective thermal paths as possible.

Considering the high thermal conductivity ($20 \text{ W m}^{-1} \text{ K}^{-1}$) of aluminum nitride (Al_2O_3), the high thermal conductivity ($170 \text{ W m}^{-1} \text{ K}^{-1}$) and the cost-effectiveness of aluminum oxide (AlN), this study optimized the thermal conductivity of silicone rubber by simultaneously incorporating 22 vol% of the two types of ceramic powders in a 1:1 ratio. By using an ionic stirrer to mix the silicone rubber and ceramic powders in a water bath at 20 °C. This modification imparts excellent thermal conductivity and low impedance in silicone rubber [30]. The composition used was optimized to enhance the thermal performance while also ensuring high mechanical properties to meet the experimental requirements. To characterize the microstructure, scanning electron microscopy (SEM) was employed for the cross-sectional analysis of the unfilled and filled silicone rubbers used in the study as shown in Fig. 7. Energy dispersive X-ray spectroscopy (EDS) results illustrate that the large particles represent Al_2O_3 and the smaller ones are AlN particles in Fig. 7(b). It can be observed that both Al_2O_3 and AlN powders are uniformly dispersed in the silicone rubber matrix, forming multiple

Table 1
Piezoelectric parameters of PZT4.

Parameter		Parameter	
C_{11}^E (10^{10} N m^{-2})	13.9	e_{31} (C m^{-2})	−5.2
C_{12}^E (10^{10} N m^{-2})	7.78	e_{33} (C m^{-2})	15.1
C_{13}^E (10^{10} N m^{-2})	7.43	e_{15} (C m^{-2})	12.7
C_{33}^E (10^{10} N m^{-2})	11.5	$\epsilon_{33}^S/\epsilon_0^S$	635
C_{44}^E (10^{10} N m^{-2})	2.56	d_{33} ($10^{-12} \text{ C N}^{-1}$)	289
C_{66}^E (10^{10} N m^{-2})	3.06	d_{31} ($10^{-12} \text{ C N}^{-1}$)	−171

Table 2
Parameters of the components in piezoelectric composites.

Material	Density (kg m ⁻³)	Specific heat capacity (J kg ⁻¹ K ⁻¹)	Thermal conductivity (W m ⁻¹ K ⁻¹)	Young's Modulus (10 ⁹ N m ⁻²)	Poisson's Ratio
PZT4	7500	420	2.1	76.5	0.32
epoxy resin	1200	550	0.8	6.3	0.3
silicon rubber	1070	1400	1.2	0.0026	0.49
aluminium alloy	2730	897	166	69	0.33

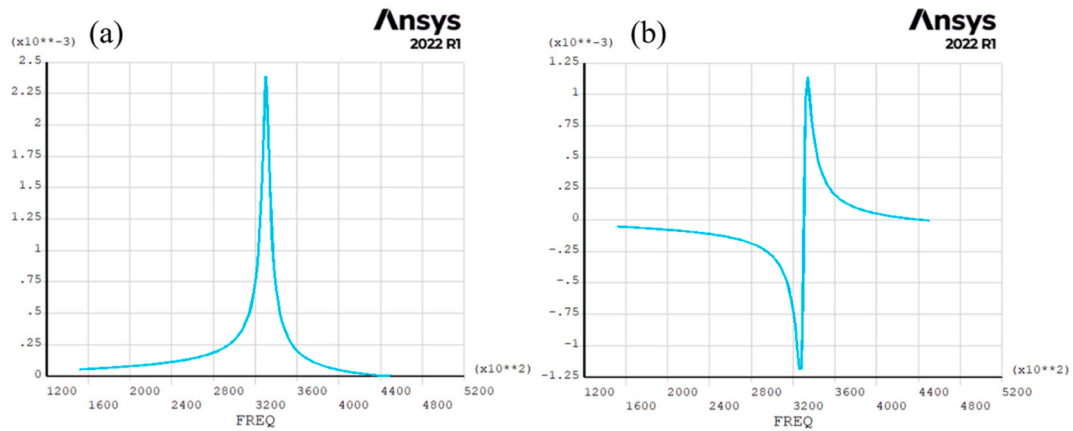


Fig. 2. (a) Simulated conductivity and (b) admittance curve of 1-1-3 piezoelectric composite.

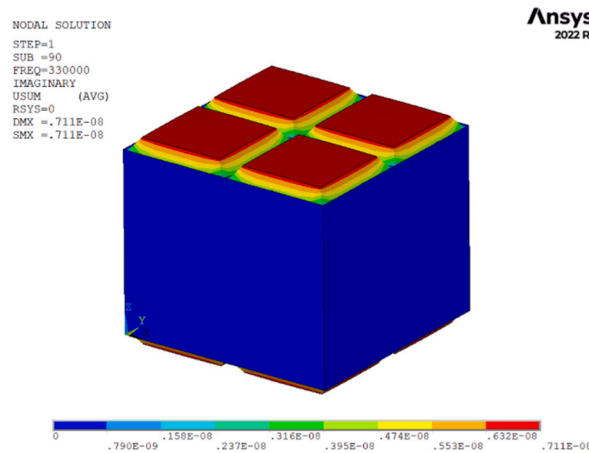


Fig. 3. Vibration diagram of 1-1-3 piezoelectric composite.

efficient paths of thermal conduction within the composite rubber suitable for enhanced thermal efficiency [31].

The preparation process of 1-1-3 piezoelectric composites is depicted in Fig. 8. In order to ensure the consistency of the resonance of each piezoelectric composite material, a complete piece of piezoelectric ceramic is been cut into piezoelectric ceramic rods which are periodic arrangement on a piezoelectric base. A metal frame which has the same periodic with piezoelectric ceramic rods. Then high thermal conductive adhesive has been poured into the gaps between the piezoelectric ceramic rods and the metal frame. After curing for more than 24 h, grinding away the remaining ceramic base. and then sputtering silver onto the upper and lower surfaces of the material to form the electrodes.

Four types of piezoelectric composites, as shown in Fig. 9, were prepared for the experimental study. Dimensions of the four piezoelectric composites is $47.7^L \times 47.7^W \times 4.5^T$ mm, while the size of the piezoelectric ceramic column is $2.22^L \times 2.22^W \times 4.5^T$ mm. Among these samples, the first (1#) and second (2#) samples were 1–3 piezoelectric composites composed of epoxy resin/PZT4 and silicone rubber/PZT4, respectively. At the same time, the third (3#) and fourth (4#) samples were 1-1-3 piezoelectric composites comprising pristine silicone rubber/aluminum alloy/PZT4 and conductive silicone rubber/aluminum alloy/PZT4, respectively.

The piezoelectric performance of the composites was measured using an Agilent 4294A impedance analyzer, and the results are

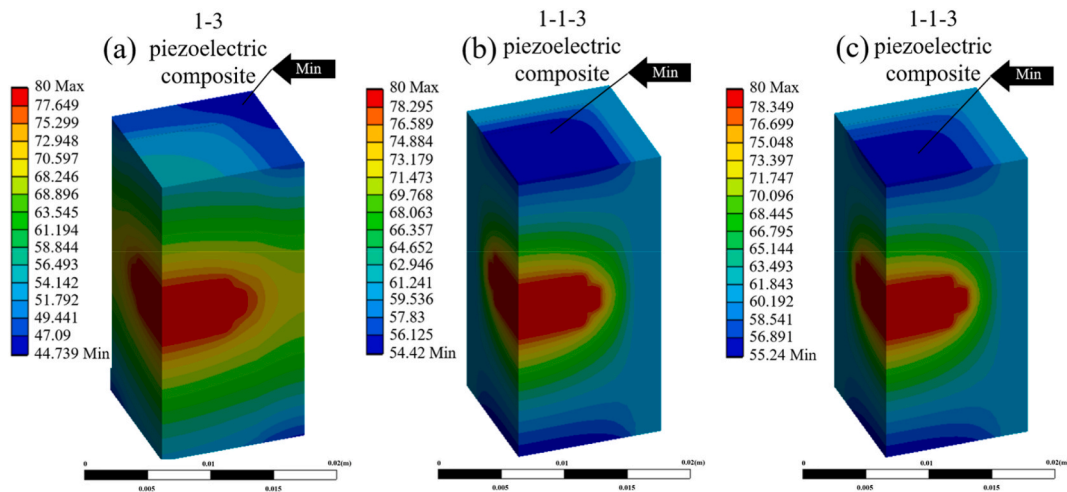


Fig. 4. Temperature distribution contour maps of piezoelectric composites with different components. (a) 1–3 piezoelectric composite composed of piezoelectric ceramic and epoxy (with thermal conductivity of $0.8 \text{ W m}^{-1} \text{ K}^{-1}$); (b) 1-1-3 piezoelectric composite composed of piezoelectric ceramic, silicone rubber (with thermal conductivity of $1.2 \text{ W m}^{-1} \text{ K}^{-1}$) and aluminum alloy; (c) 1-1-3 piezoelectric composite composed of piezoelectric ceramic, silicone rubber (with thermal conductivity $1.8 \text{ W m}^{-1} \text{ K}^{-1}$) and aluminum alloy.

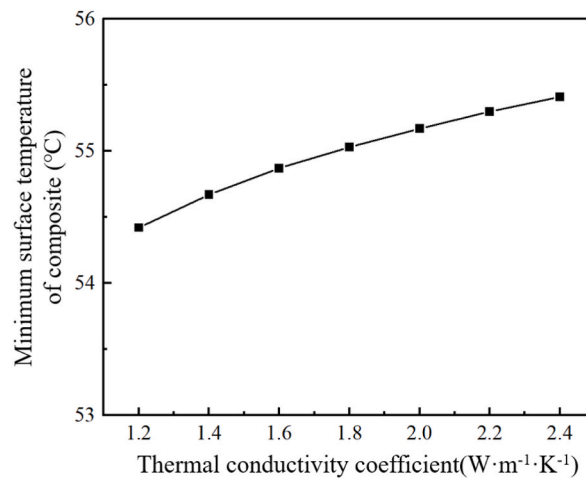


Fig. 5. Minimum temperature on the surface of 1-1-3 composite as a function of thermal conductivity of the silicone rubber.

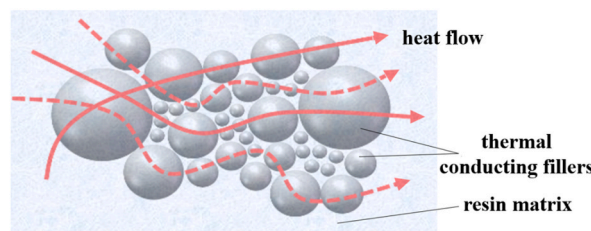


Fig. 6. Microscopic heat conduction paths in modified silicone rubber.

presented in Table 3 and Fig. 10. By comparing and analyzing the recorded data, a close similarity was observed in the series resonance frequency and parallel resonance frequency of the four composites. It can, therefore, be concluded that all the composites possessed comparable piezoelectric performance.

In order to further explore the temperature stability of the piezoelectric composites, the electrical properties of the samples were tested at 30°C , 50°C , 70°C , 90°C , 110°C , 150°C after keeping 20 min in an oven. The conductivity curves of piezoelectric composites

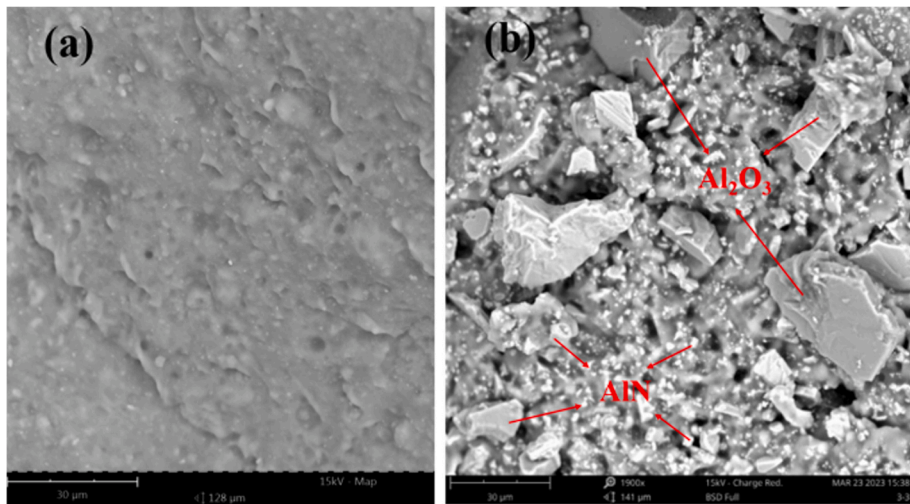


Fig. 7. SEM images of silicon rubbers: (a) Pristine and (b) Filled with Al_2O_3 and AlN powders.

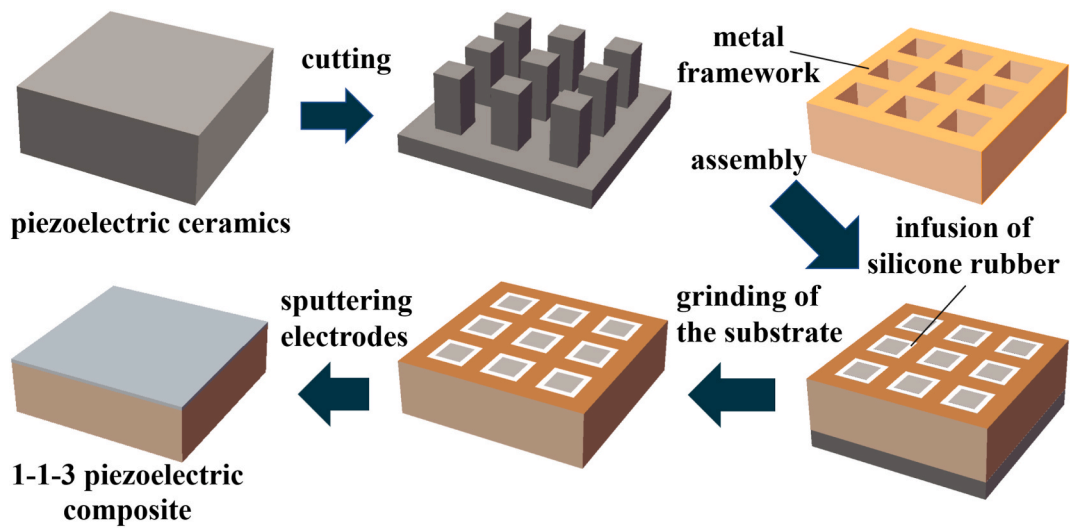


Fig. 8. Preparation process diagram of 1-1-3 piezoelectric composites.

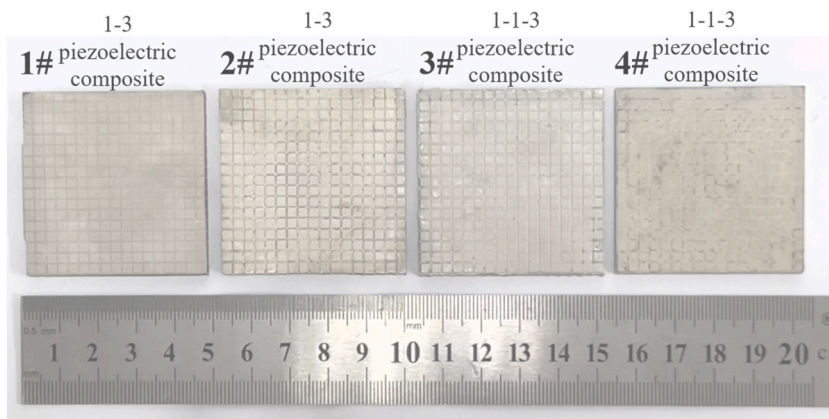


Fig. 9. Digital photographs of the piezoelectric composites.

Table 3
Performance parameters of the piezoelectric composites.

Sample	Resonant Frequency f_s (kHz)	Anti-resonant Frequency f_p (kHz)	Electromechanical Coupling Factor k_t	Bandwidth (kHz)	Mechanical Quality Factor
1#	328	419	0.622	4.1	78
2#	322	425	0.653	6.8	48
3#	325	414	0.619	7.6	43
4#	325	415	0.622	7.2	45

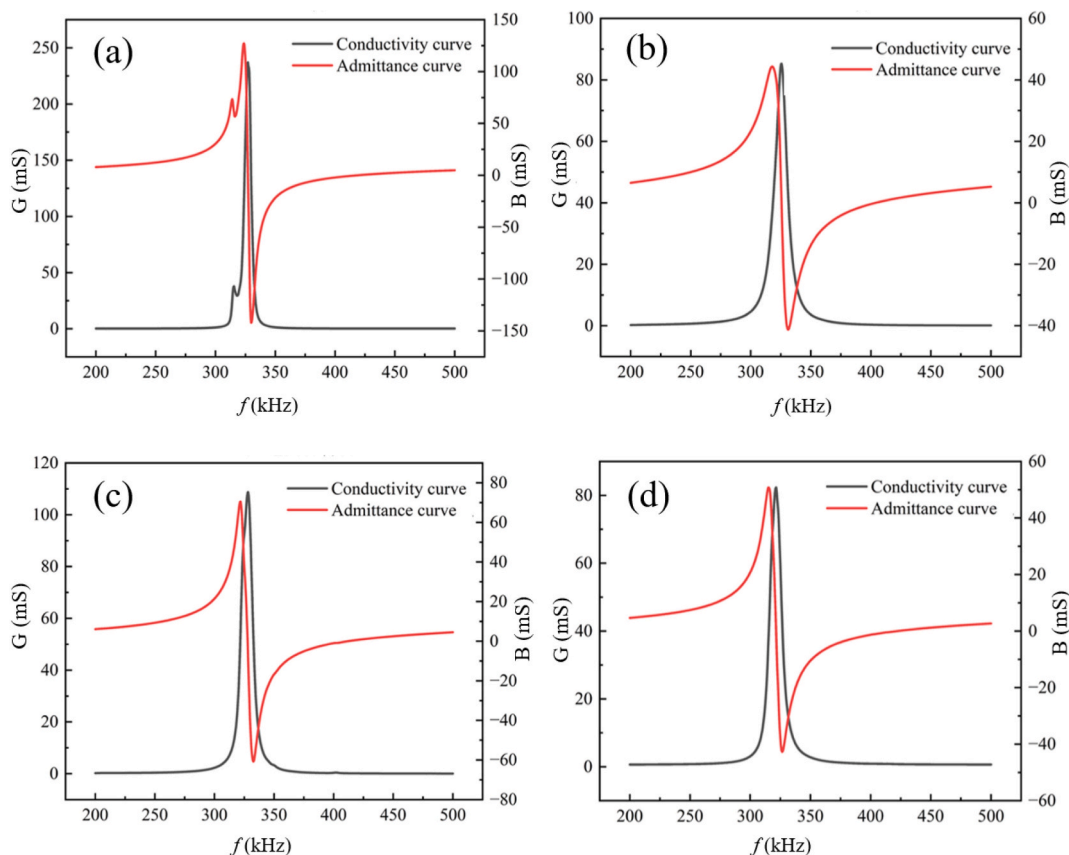


Fig. 10. Admittance and conductivity curves of the piezoelectric composites: (a) 1#, (b) 2#, (c) 3# and (d) 4#.

are shown in Fig. 11. It can be seen that the resonant frequencies of composite 2#, 3# and 4# shifted to higher frequency and the conductance at resonant frequency gradually increased by increasing the temperature. And all these three kinds of composite show the same trends. By comparing the frequency shift and the conductance increasing for composite 2#, 3# and 4#, it can be seen that composite 4# shows more temperature stability by introducing highly thermally conductive structure. But the composite 1#, shows different trend. First of all, it has an interference peak before the main harmonic peak which always appears in 1–3 composite, when the temperature is lower than 90 °C. It is due to the strong coupling effect caused by resin epoxy. We think the 90 °C is the glass transition temperature of this kind of epoxy resin. Second, for composite 1#, the resonant frequencies shifted to lower frequency by increasing the temperature. For 1–3 composite, the frequency shift is mainly caused by the epoxy resin. Meanwhile, for 1–3 composite, the frequency shift is mainly caused by the epoxy resin piezoelectric ceramic.

The relationship between electromechanical coupling coefficients and temperatures of four piezoelectric composites are presented in Fig. 12, which showed the same trends with frequency shift. The electromechanical coupling coefficients of composite 2#, 3# and 4# decreases with increasing temperature and the composite #1 is on the contrary.

An elevated temperature rate test was employed to validate the thermal conductivity performance of each composite. The temperature rate test was conducted on a heating platform, with the heating temperature set to 80 °C. As depicted in Fig. 13, the sides of the four composites were placed on the heating platform, and their real-time surface temperature was monitored by a thermal imaging camera (model: FLIR T560). As reflected by the real-time imaging, the heat was transferred from the surface of the heating table to the bottom of each composite, from where it was conducted inside the material.

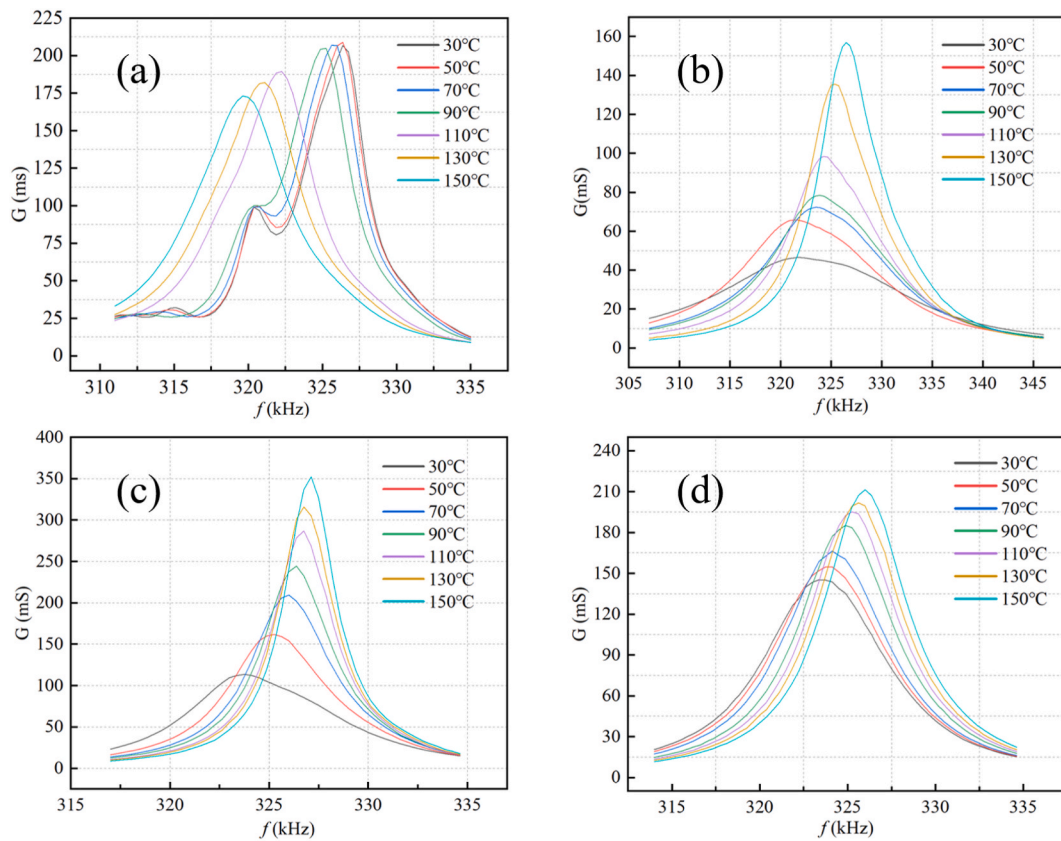


Fig. 11. Conductivity curves of four composites at different temperatures: (a) 1 # piezoelectric composite, (b) 2 # piezoelectric composite, (c) 3# piezoelectric composite, (d) 4 # piezoelectric composite.

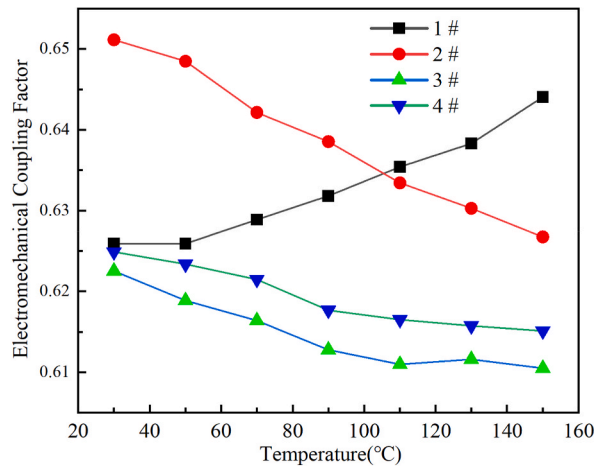


Fig. 12. Relationship between electromechanical coupling coefficients and temperatures of four piezoelectric composites.

Considering temperature measurement errors, the study considered the real-time monitoring of the average temperature at the same height and within the same area of each composite. These real-time recorded temperatures were plotted, as illustrated in Fig. 14, for comparison. A rapid rise in temperature within the first 100 s was a common feature of the four types of composites, with the average temperature changing from 15 °C to 22.5 °C, 14.5 °C–22 °C, 15 °C–36.7 °C, and 15 °C–38.8 °C for composite 1#, 2#, 3# and 4#, respectively. This rising temperature finally stabilized after 600 s, with composite 1#, 2#, 3#, and 4# reaching 32.6 °C, 34.6 °C, 50.0 °C, and 50.7 °C, respectively.

The experiment results, therefore, indicated that the novel piezoelectric 1-1-3 composite exhibited a temperature increase rate

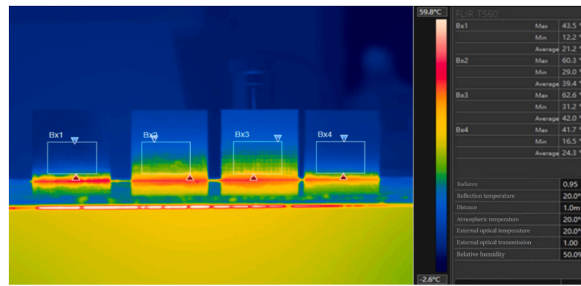


Fig. 13. Real-time thermal imaging of the piezoelectric composites.

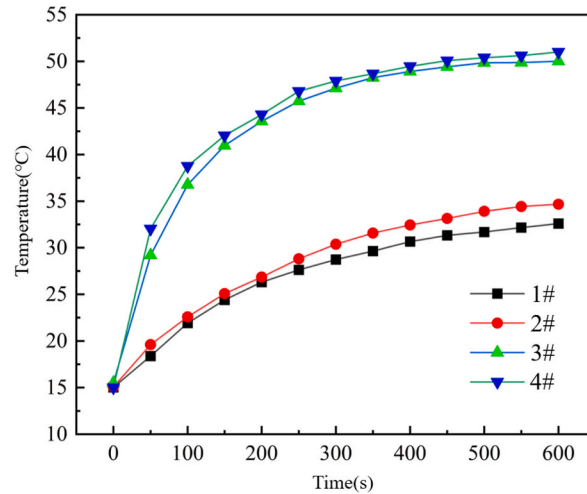


Fig. 14. Real-time temperature change in the piezoelectric composites.

approximately three times faster than the conventional 1–3 piezoelectric composite in the initial time phase. Moreover, its heating efficiency was about twice as high as that of the conventional composite. Thus, the 1-1-3 piezoelectric composite designed in this study demonstrated excellent piezoelectric performance while efficiently conducting heat from within the ceramic core.

For verifying the actual effect of this thermally conductive structure, two transducers were prepared as shown in Fig. 15. Conventional transducer (CT) with 1–3 piezoelectric composite was composed of PZT4/epoxy resin as the core. Efficient heat dissipation transducer (EHDT) with the novel 1-1-3 piezoelectric composite as the core which was composed of PZT4/conductive silicone rubber and copper frame, and combining heat pipe-fin heat dissipation structure. The parameters of the two transducers are shown in Table 4. The transmitting voltage response (TVR) of the two transducers are shown in Fig. 16. It showed the TVR of CT and EDHD reached 177.1 dB and 171.1 dB respectively at 260 kHz.

Series heat dissipation experiments were conducted to verify the heat dissipation performance of these two transducers. In this

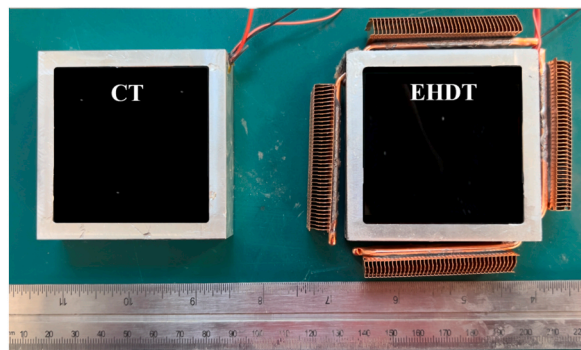


Fig. 15. Photos of CT and EHDT

Table 4
Performance parameters of CT and EHDT.

Type	Resonant Frequency f_s (kHz)	Anti-resonant Frequency f_p (kHz)	Electromechanical Coupling Factor k_t	Bandwidth (kHz)	Mechanical Quality Factor
CT	261	326	0.599	3.1	84
EHDT	259	330	0.619	7.6	34

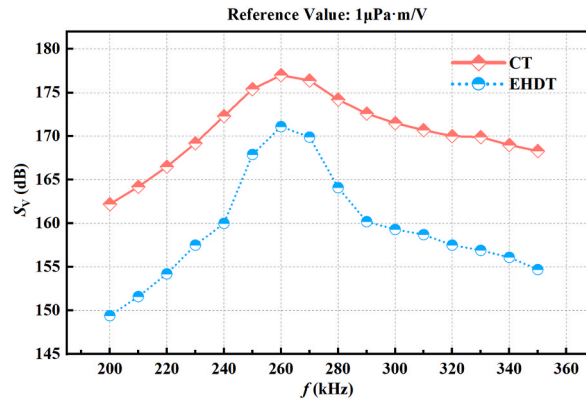


Fig. 16. Transmit voltage response of CT and EHDT.

paper, a K-type thermocouple probe is placed in the center of the surface of piezoelectric composites in both CT and EDHD. First, the two transducers were driven by a 20 W continuous sine signal at 260 kHz respectively for 180s. The temperature changes with time of CT and EHDT are shown in Fig. 17. The CT’s temperature rises from 20 °C to 76 °C within 180s. And the temperature has almost the same rising rate within 180s. The temperature of EHDT reached 36 °C within 30s. And then the temperature gets steady about 33 °C for the next 150s.

Second, dynamic temperature test has been performed by applying different electrical input powers. The internal temperatures of these two transducers have been test after driven by continuous sine signal at 260 kHz for 180s respectively. The internal temperatures curves varying with electrical input power is shown in Fig. 18. The test results showed that the internal temperature is always under the threshold of 90 °C, when the input power is up to 100 W. At the meanwhile, the internal temperature of CT gets up to 95 °C, when the input power is only 30 W. Obviously, the efficient heat dissipation transducer has excellent heat dissipation performance and relief the heat accumulation inside conventional transducers effectively.

5. Conclusion

A novel highly thermally conductive 1-1-3 piezoelectric composite was designed and prepared. This composite material utilized PZT-4 piezoelectric ceramics as one phase while silicone rubber with added Al₂O₃ and AlN fillers as the other. The highly conductive fillers established internal heat conduction paths within the insulating silicone matrix, thus enhancing its heat dissipation efficiency. Additionally, an aluminum alloy framework was used as the third phase of the composite to further improve efficiency. This design

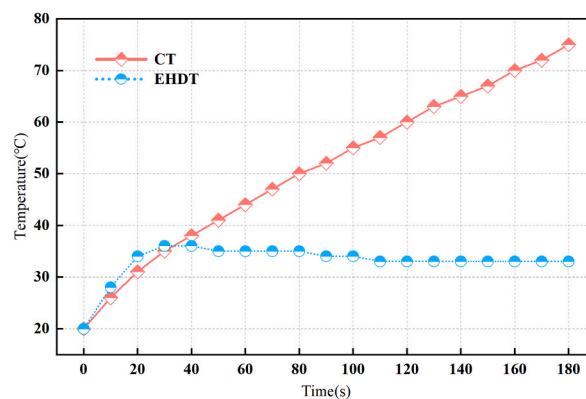


Fig. 17. Internal temperature change of CT and EHDT.

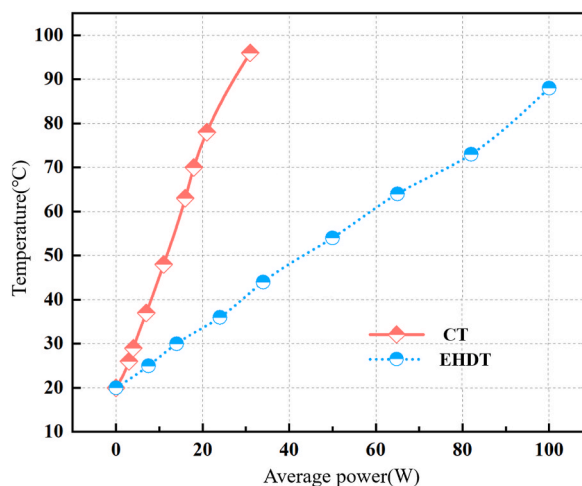


Fig. 18. Relationship between input power and temperature of transducers.

significantly enhanced the thermal conductivity of the material while ensuring high strength and piezoelectric performance. After heating for 600 s, the temperature rise remained nearly twice that of the 1–3 piezoelectric composite. Compared with conventional 1–3 piezoelectric composite, the novel 1-1-3 piezoelectric composite shows greatly improved thermal conduction while maintaining the same piezoelectric properties. A new highly thermally conductive transducer was designed and fabricated, which used the new 1-1-3 piezoelectric composite as the core and combined heat pipe-fin heat dissipation structure. The new 1-1-3 piezoelectric transducer can work under three times more power than the conventional 1–3 piezoelectric transducer at the temperature threshold of 90 °C.

Data availability statement

The data that support the findings of this study are available on request from the corresponding author, upon reasonable request.

Funding

This work was supported by National Natural Science Foundation of China (U2006218). This work was also supported by The Project of Construction and Support for high-level Innovative Teams of Beijing Municipal Institutions (BPHR20220124).

CRediT authorship contribution statement

Zhiyang Liu: Writing – original draft, Validation, Methodology, Data curation. **Zhiwei Zhang:** Writing – review & editing, Methodology, Data curation. **Lei Qin:** Writing – review & editing, Supervision, Project administration, Methodology, Funding acquisition.

Declaration of competing interest

The authors declare the following financial interests/personal relationships which may be considered as potential competing interests: Lei Qin reports financial support was provided by Beijing Information Science & Technology University. If there are other authors, they declare that they have no known competing financial interests or personal relationships that could have appeared to influence the work reported in this paper.

References

- [1] J. Xu, Z. Han, N. Wang, Z. Li, J. Lv, X. Zhu, Y. Jian X. Cui, Micromachined high frequency 1–3 piezocomposite transducer using picosecond laser, *IEEE Trans. Ultrason. Ferroelectrics Freq. Control* 68 (6) (2021) 2219–2226.
- [2] S. Hao, C. Zhong, Y. Zhang, Y. Wang L. Chen, L. Qin, Flexible 1-3 piezoelectric composites with soft embedded conductive interconnects for underwater acoustic transducers, *ACS Appl. Electron. Mater.* 5 (5) (2023) 2686–2695.
- [3] D. Chen, C. Hou, C. Fei, D. Li, P. Lin, J. Chen, Y. Yang, An optimization design strategy of 1–3 piezocomposite ultrasonic transducer for imaging applications, *Mater. Today Commun.* 24 (2020) 100991.
- [4] H. Jae Lee, S. Zhang, X. Geng, T.R. Shrout, Electroacoustic response of 1-3 piezocomposite transducers for high power applications, *Appl. Phys. Lett.* 101 (2012) 25.
- [5] Zhongzheng Liu, Tao Zhang, Yanzhang Geng, An Tong, Underwater wireless high-efficiency energy transmission method based on the ultrasonic transducer array. 2021 IEEE 21st International Conference on Communication Technology (ICCT), IEEE, 2021.
- [6] S.A.H. Mohsan, M.A. Khan, A. Mazinani, M.H. Alsharif, H.S. Cho, Enabling underwater wireless power transfer towards sixth generation (6g) wireless networks: opportunities, recent advances, and technical challenges, *J. Mar. Sci. Eng.* 10 (9) (2022) 1282.

- [7] X. Yi, W. Zheng, H. Cao, et al., Wireless power transmission for implantable medical devices using focused ultrasound and a miniaturized 1-3 piezoelectric composite receiving transducer, *IEEE Trans. Ultrason. Ferroelectrics Freq. Control* 68 (12) (2021) 3592–3598.
- [8] Olumide Alamu, Thomas O. Olwal, Karim Djouani, Energy harvesting techniques for sustainable underwater wireless communication networks: a review. *E-Prime-Advances in Electrical Engineering, Electronics and Energy*, 2023 100265.
- [9] Chakridhar Reddy Teeneti, Tadd T. Truscott, David N. Beal, Zeljko Pantic, Review of wireless charging systems for autonomous underwater vehicles, *IEEE J. Ocean. Eng.* 46 (1) (2019) 68–87.
- [10] D. Thomas, D.D. Ebenezer, S.M. Srinivasan, Power dissipation and temperature distribution in piezoelectric ceramic slabs, *J. Acoust. Soc. Am.* 128 (4) (2010) 1700–1711.
- [11] Luan Guidong, Jinduo Zhang, Renqian Wang, *Piezoelectric Transducer and Transducer Array*, the Press of Perking University, Beijing, 2005.
- [12] Hyeong Jae Lee, Shujun Zhang, Design of low-loss 1-3 piezoelectric composites for high-power transducer applications, *IEEE Trans. Ultrason. Ferroelectrics Freq. Control* 59 (9) (2012) 1969–1975.
- [13] W. Wang, R. Liang, Z. Zhou, Y. Zhang, X. Dong, Defect engineering for reduced large AC signal dielectric loss of PZT-based hard piezoelectric ceramics, *J. Am. Ceram. Soc.* 105 (1) (2022) 279–291.
- [14] Li Yingwei, Zhou Xilong, Li Faxin, Experimental study on high-temperature deformation and failure of PZT piezoelectric ceramics, *Exp. Mech.* 27 (5) (2012) 527–534.
- [15] Junjie Shan, Wang Sha, Fan Zhou, Lingzhi Cui, Yanfeng Zhang, Zhongfan Liu, Enhancing the heat-dissipation efficiency in ultrasonic transducers via embedding vertically oriented graphene-based porcelain radiators, *Nano Lett.* 20 (7) (2020) 5097–5105.
- [16] R. Zhang, Z. Liu, Z. Sun, A scalable highly thermal conductive silicone rubber composite with orientated graphite by pre-vulcanizing and multilayer stacking method, *Compos. Appl. Sci. Manuf.* 157 (2022) 106944.
- [17] D. Thomas, D.D. Ebenezer, S.M. Srinivasan, Power dissipation and temperature distribution in piezoelectric ceramic slabs, *J. Acoust. Soc. Am.* 128 (4) (2010) 1700–1711.
- [18] Y. Yao, Y. Pan, S. Liu, Study on heat pipe heat dissipation of high-power ultrasonic transducer, *Ultrasonics* 120 (2022) 106654.
- [19] N. Mehra, L. Mu, T. Ji, X. Yang, J. Kong, J. Gu, J. Zhu, Thermal transport in polymeric materials and across composite interfaces, *Appl. Mater. Today* 12 (2018) 92–130.
- [20] W. Chen, Hydrodynamic heat transfer in solids, *Int. J. Heat Mass Tran.* 215 (2023) 124455.
- [21] C. Sun, C. Zhong, L. Wang, L. Qin, Design and preparation of double-harmonic piezoelectric composite lamination, *Materials* 15 (22) (2022) 7959.
- [22] C. Zhong, L. Wang, L. Qin, Y. Zhang, Characterization of an improved 1-3 piezoelectric composite by simulation and experiment, *J. Appl. Biomater. Funct. Mater.* 15 (1_suppl) (2017) 38–44.
- [23] Yanjun Zhang, Likun Wang, Lei Qin, Equivalent parameter model of 1-3 piezocomposite with a sandwich polymer, *Results Phys.* 9 (2018) 1256–1261.
- [24] R. Sun, L. Wang, Y. Zhang, C. Zhong, Characterization of 1-3 piezoelectric composite with a 3-tier polymer structure, *Materials* 13 (2) (2020) 397.
- [25] J. Zhang, J. Wang, C. Zhong, L. Qin, 1-3-Type piezoelectric composites with three-layer cascade structure, *Compos. Struct.* 322 (2023) 117406.
- [26] Lei Qin, Junbo Jia, Minkyu Choi, Kenji Uchino, Improvement of electromechanical coupling coefficient in shear-mode of piezoelectric ceramics, *Ceram. Int.* 45 (2) (2019) 1496–1502.
- [27] Xuhui Mi, Lei Qin, Qingwei Liao, Likun Wang, Electromechanical coupling coefficient and acoustic impedance of 1-1-3 piezoelectric composites, *Ceram. Int.* 43 (9) (2017) 7374–7377.
- [28] Yanfei Xu, Xiaojia Wang, Hao Qing, A mini review on thermally conductive polymers and polymer-based composites, *Compos. Commun.* 24 (2021) 100617.
- [29] Alok Agrawal, Alok Satapathy, Development of a heat conduction model and investigation on thermal conductivity enhancement of AlN/epoxy composites, *Procedia Eng.* 51 (2013) 573–578.
- [30] H.T. Chiu, T. Sukachonmakul, M.T. Kuo, Y.H. Wang, K. Wattanakul, Surface modification of aluminum nitride by polysilazane and its polymer-derived amorphous silicon oxycarbide ceramic for the enhancement of thermal conductivity in silicone rubber composite, *Appl. Surf. Sci.* 292 (2014) 928–936.
- [31] Seran Choi, Jooheon Kim, Thermal conductivity of epoxy composites with a binary-particle system of aluminum oxide and aluminum nitride fillers, *Compos. B Eng.* 51 (2013) 140–147.